Conference on Bluff Body Wakes and Vortex-Induced Vibrations (BBVIV3)
Port Douglas, Australia
17-20 December, 2002

Low Frequency Unsteadiness in the Wake of Elliptical Cylinders

S.A. Johnson, M.C. Thompson and K. Hourigan

Department of Mechanical Engineering
Monash University, Clayton, Victoria, 3800 AUSTRALIA

Abstract

The vortex structures behind 2D elliptical cylinders at low Reynolds numbers were investigated for a Reynolds numbers range of 75 to 175. By varying the aspect ratio of an elliptical cylinder, the geometry is varied between the extremes of a circular cylinder and a flat plate normal to the flow. The power spectrum frequency analysis of the horizontal centre line y-velocity was conducted and showed the presence of secondary and tertiary frequencies in the far region of the wake. The results show that as the Reynolds number is increased and/or the aspect ratio is decreased, the lower frequencies in the far wake become more dominant and their inception point occurs closer to the elliptical cylinder. Results also show that if the primary structures decay before the secondary frequencies become dominant, there are no secondary structures observed in the far wake region. This research indicates that the low frequency unsteadiness behind normal flat plates was not due to the vortex interaction, but, rather, due to the presence of a two-dimensional instability occurring close to the plate.

Introduction

Flow structures behind bluff bodies have been the focus of extensive research due to their importance to the drag on vehicles and structures. The circular cylinder has been the benchmark bluff body used for the majority of research. However, at low Reynolds numbers (Re), the low frequency unsteadiness that is observed behind normal flat plates is not present. The wakes of elliptical cylinders enable the analysis of large structures that occur in the far wake because they form closer to the body before they are diffused.

Najjar and Balachandar [3] conducted two-dimensional (2D) and three-dimensional (3D) simulations on a normal flat plate at Re=250 investigating low frequency unsteadiness. In the 2D simulations, the drag coefficient exhibited a dominant periodic cycle driven by the shedding of Karman type vortices. However, a low frequency component was apparent in the time history of the drag coefficient. Najjar and Balachandar stated that the Karman vortex interaction downstream caused the low frequency unsteadiness. This kind of periodic behaviour was not observed in the 3D simulation. The mechanism responsible for low frequency unsteadiness was due to a gradual switching back and forth between shedding cycles of high mean and low mean drag. The high drag regime structure resembled a mode B-type shedding structure [9], while the low drag wake resembled a large-scale dislocation similar to that observed behind circular cylinders [8]. The 2D simulations were largely ignored by Najjar and Balachandar, even though low frequency unsteadiness was present because the wake structures were so different from the 3D results.

Few papers have explored flow structures in the far wake which are different from those observed in the near wake region. Visualisations made by Taneda [4] showed the decay of the Karman street wake and the growth of a larger secondary structure in the far wake that appeared to be much like the original Karman vortex street, but on a larger scale. Taneda concluded that the secondary vortex street was due a hydrodynamic instability based on the mean velocity profile in which the original structure decays and the wake 'rearranges' itself into a new configuration appropriate to the new downstream position. Cimbala et al. [1] concluded that the secondary wake structure did not depend on the scale or frequency of the Karman shedding frequency. Their results showed that the frequencies amplified in the far wake were not related to the Karman shedding frequency but had good agreement to those found using linear stability theory. Conversely, Williamson [6] demonstrated that the far wake was extremely sensitive to free-stream disturbances and that the near wake (FK) frequency directly influenced the far wake. The frequency of the far wake (FFW) was given by FFW = FK - FT where FT was the frequency of two-dimensional instability. As a result of free stream disturbances, it was very difficult to define a natural wake state since it was dependent on the experimental conditions.

This paper examines the nominally two-dimensional wake states behind elliptical bodies using numerical simulation as the body geometry changes from a flat plate normal to the free stream flow to that of a circular cylinder. In particular, it is concerned with secondary and tertiary structures in the wake and their associated frequencies. A revised parameter space model for the wake structures [2] is outlined and the frequency power spectrum graphs are analysed.

The two parameters that were varied in this investigation were the Aspect Ratio (AR) and Reynolds number (Re). Shown in Figure 1 is the progression of a flat plate to a cylinder where AR=B/A. Therefore, a vertical flat plate has an AR=0 while for a circular cylinder, AR=1. The transverse width (A) is used as the Re length scale for the simulations.

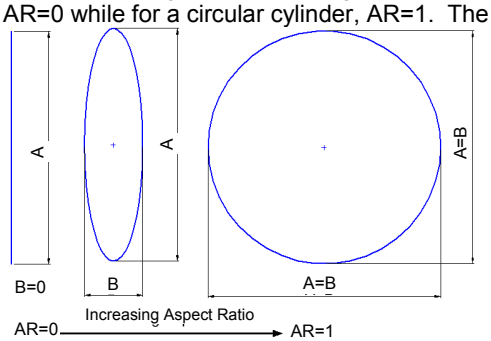

Figure 1: Schematic diagram of changing aspect ratio. Shown is AR=0.01, AR=0.25, and AR=1.0

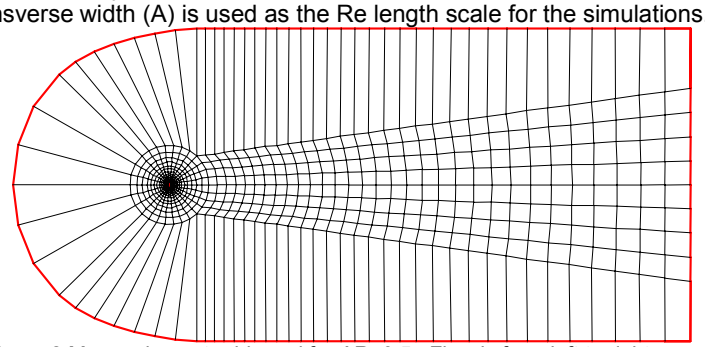

Figure 2 Macro element grid used for AR=0.5. Flow is from left to right. Origin of the axis is located in the centre of the cylinder. More information of the grid setup can be found in [2]. Outlet is 100 non dimensional units (NDU) downstream from the elliptical cylinder.

A 2D spectral-element method [5] was used to solve the unsteady Navier-Stokes equations governing the fluid flow. Simulations were carried out for AR=0.01 to 1.00 and for Re=75 to 175. The numerical grid is displayed in Figure 2.

Results

Data Collection Method

To conduct the analysis of the frequency response, simulations were run until all transient effects were removed from the domain. A time history of the X and Y velocity components at 46 discrete points behind the elliptical cylinder on the horizontal centre line was logged until there was enough data for at least a 2^{18} point fast Fourier transform (FFT). The power spectrum from the time series of the Y component of velocity was used to determine the dominant frequencies present in the wake.

Shedding Patterns

The six shedding patterns previously outlined by Johnson [2] have been remapped to five flow structures which have clear boundaries according to the frequency power spectrum along the centre line. These are categorised as the no frequency (F0), primary frequency (F1), secondary frequency with no interaction (F2NI), secondary frequency (F2) and low frequency (LF) regimes. The F0 regime is not discussed in this paper, as there is no associated shedding frequency but is discussed in Johnson [2].

The F1 regime consists of Karman type vortex shedding patterns in the wake of the cylinder. As shown in Figure 3, in the far wake region, positive and negative vortex cores diffuse together into two rows extending downstream to the outlet. These two shear layers are symmetric about the horizontal centreline.

In the F2NI regime, a two dimensional instability is present in the far wake. However, in the region where the secondary frequency is present, the primary shedding from the cylinder has decayed sufficiently such that it does not interact with the Karman vortices and no secondary structures are observed. The flow field visualisations are the same as those for the F1 regime (Figure 3).

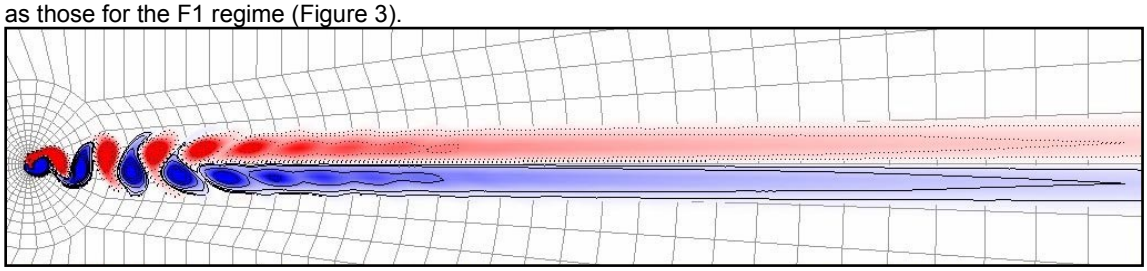

Figure 3 Primary frequency (F1) regime at Re=075 for AR=0.25

In the F2 region, the two dimensional instability interacts with vortex structures from the primary frequency regime and secondary periodic structures are formed as shown in Figure 4. When the Re is increased, the two dimensional instability intensifies so the initiation point of the secondary structures occurs further upstream.

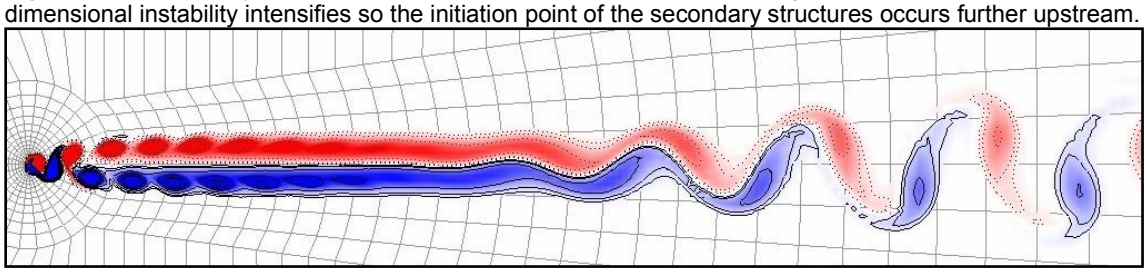

Figure 4 Secondary frequency (F2) regime at Re=125 for AR=0.25

The instantaneous plot of the vorticity in low frequency (LF) regime is illustrated in Figure 5. This regime is defined by the presence of a low frequency structure (F<0.03) in the power spectrum analysis. The flow structures are quite complex, showing several different features. In the near wake region, The Karman vortex street is quickly transformed into an unsteady secondary structure where a secondary lower frequency is dominant. At higher Reynolds numbers (Re>150 for AR=0.25), a tertiary frequency dominates the far wake flow field. Flow visualisation animations show the vortex structures starting to interact to form a larger structure encompassing the smaller vortices. The corresponding wavelength of the two dimensional instability is visualised in Figure 5 by a dashed line passing through the vortex pairs in the wake. It is this low frequency structure interacting with the von Karman street that causes the secondary and tertiary structures and associated frequencies in the wake.

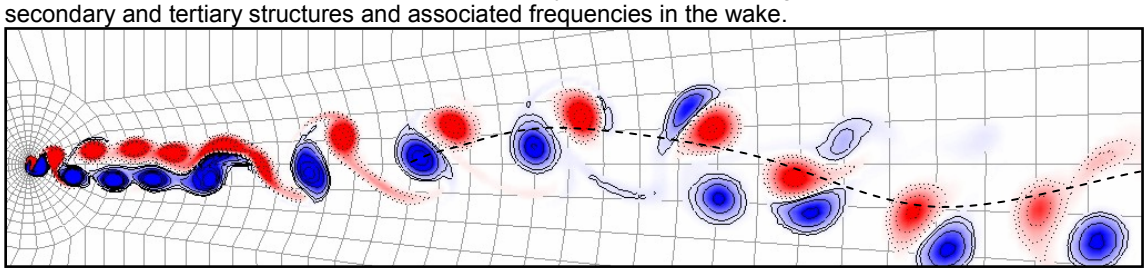

Figure 5 Low frequency (LF) regime at Re=175 for AR=0.25

Parameter Space Map.

The parameter space model depicting the regions where various regimes occur is shown in Figure 6. For high AR and low Re, the F1 regime is present in the wake. As the AR decreases and/or the Re increases, the wake moves through the F2NI regime until the secondary frequency interacts with the primary frequency in the F2 regime. For high Re and low AR, the low frequency structure is present causing unsteady secondary shedding and tertiary shedding. Since the outlet boundary is located 100 NDU downstream, any frequencies amplified past 100 NDU are not included in this parameter space map.

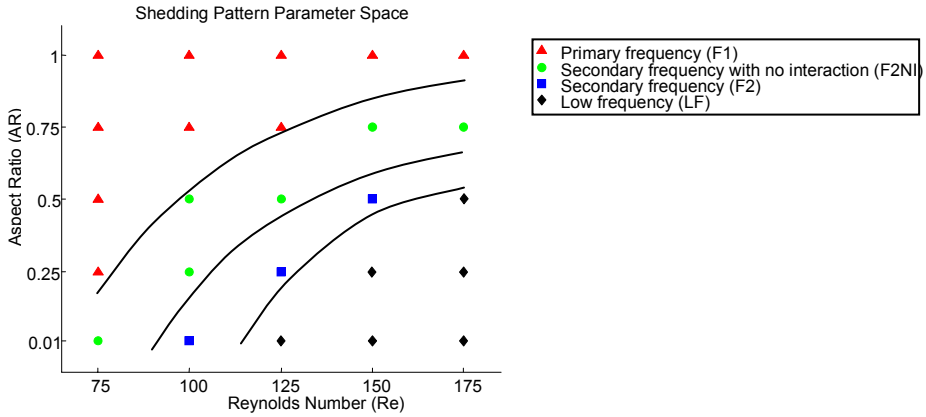

Figure 6 Shedding Pattern Parameter Space map. Solid lines are included to aid visualisation of boundaries of regimes.

Frequency Power Spectrum Analysis

The wake transition that results from the Re increase and/or the AR decrease corresponds with a change in the frequencies present in wake. The frequencies for AR=0.25 will be examined below to investigate the flow changes from the F1 to the LF regime as the Re increases. Two figures are displayed for each Reynolds number. In the top figure, the frequency power spectrum for the centre line is delineated by shaded contours of frequency power magnitude. On the X-axis is the downstream distance, with the elliptical cylinder located at X=0 NDU, and on the Y-axis is the frequency. Dark areas on the plot indicate a frequency range where the power magnitude of the given frequency is dominant. The dominant frequency at each location is indicated by a dot. The bottom figure for each Re represents the frequency amplitude versus the downstream distance of the dominant frequencies present in the wake.

As shown in Figure 7, at Re=75, only one frequency is present. This frequency is the primary frequency of the Karman vortex shedding from the elliptical cylinder, which has decayed at X≈40 NDU (Figure 10).

At Re=100 (Figure 8), a second frequency from the two dimensional instability is present in the far wake, and it is amplified as it propagates downstream. However, no secondary shedding is visible in the far wake because the primary shedding has decayed before the two-dimensional instability is strong enough to influence the wake (Figure 11).

At Re=125 (Figure 9), the amplitude of the secondary frequency is larger, and its growth initiation point has moved further upstream. The secondary shedding visible in the far wake region (Figure 4) is periodic.

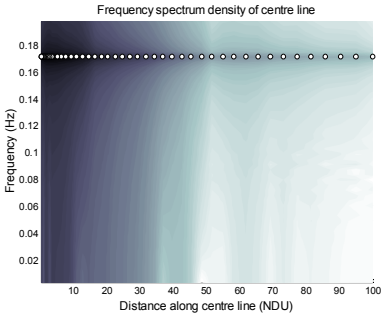

Figure 7 AR=0.25 Re=75 Frequency spectral magnitude on centre line

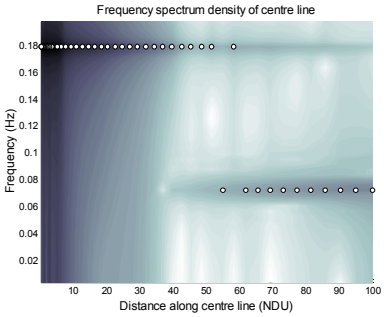

Figure 8 AR=0.25 Re=100 Frequency spectral magnitude on centre line

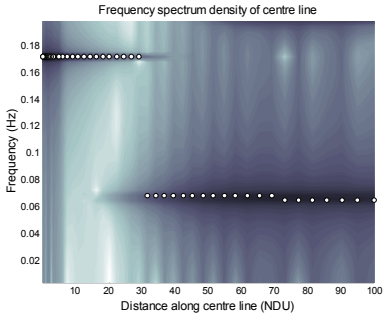

Figure 9 AR=0.25 Re=125 Frequency spectral magnitude on centre line

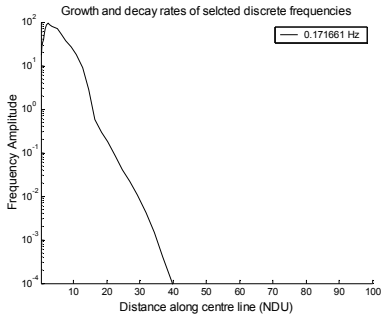

Figure 10 AR=0.25 Re=75 Dominant frequency amplitude Vs distance

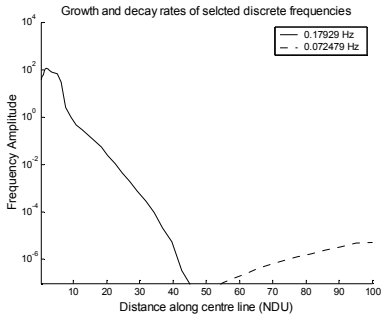

Figure 11 AR=0.25 Re=100 Dominant frequency amplitude Vs distance

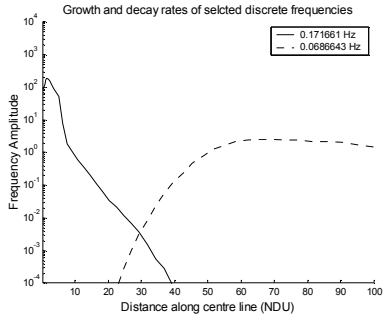

Figure 12 AR=0.25 Re=125 Dominant frequency amplitude Vs distance

When the Re is increased to 150 (Figure 13), the secondary shedding in the wake is no longer periodic because the interaction between the low frequency and the primary frequency causes the secondary frequency. This is apparent in Figure 13 where the dominant frequency in the far wake is a harmonic of the low frequency and there is a broader frequency band in the far wake region, indicating that no regular shedding pattern is present. However, the secondary frequency remains dominant at this Re (Figure 15).

As shown in Figure 14, at Re=175, three dominant frequencies are present. Between X=0 and X=12, the primary frequency is the most dominant frequency due to the vortex shedding from the elliptical cylinder. Above X=12, the vortices collapse on each other due to influence of the secondary frequency. As shown in Figure 14 and Figure 16, the tertiary frequency becomes dominant above X=70. Both the secondary and tertiary frequencies are harmonics of the low frequency. The change in dominant frequency induces secondary structures in the wake to form larger scale structures.

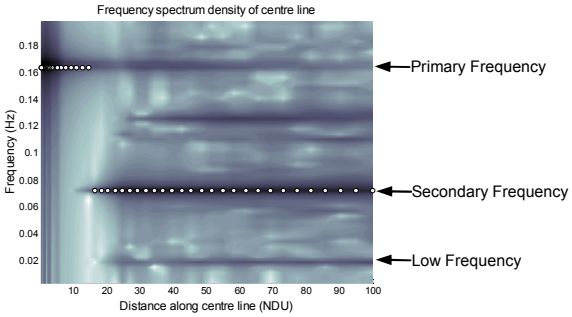

Figure 13 AR=0.25 Re=150 Frequency spectral magnitude on centre line.

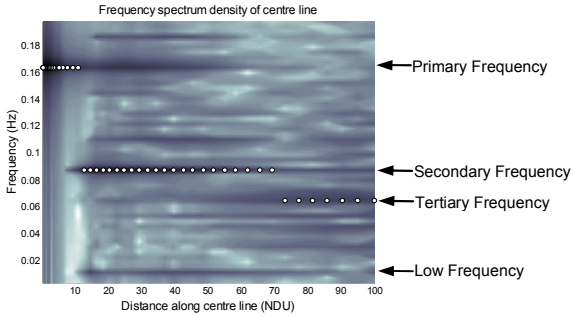

Figure 14 AR=0.25 Re=175 Spectral density on centre line.

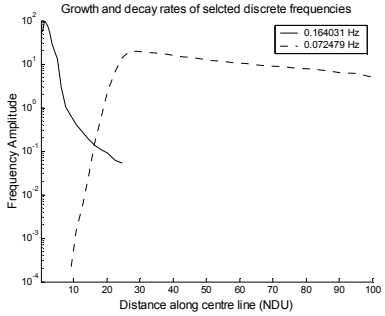

Figure 15 AR=0.25 Re=150 Dominant frequency amplitude Vs distance.

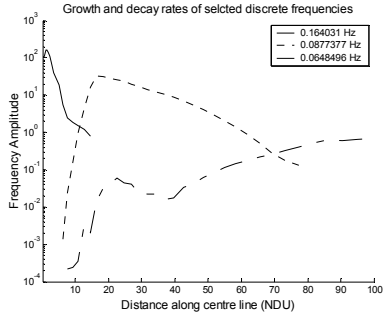

Figure 16 AR=0.25 Re=175 Dominant frequency amplitude Vs distance.

Conclusion

This paper has presented the frequency power spectra for the centreline wakes of the flow around an elliptical cylinder with varied AR and Re values. It has been shown that, as the AR is decreased and/or the Re is increased, low frequency two-dimensional structures appear in the far wake. The frequency spectrum density plots indicate that the flow structures are evolving into larger scale structures with associated lower frequencies.

These results demonstrate that the low frequency unsteadiness found in the 2D simulations by Najjar and Balachandar [3] was not due to the vortex interaction, but, rather, due to a two-dimensional instability that has been observed in the far wake [7] interacting with the vortices shed from the flat plate.

Similar to experimental results by Williamson [6], low frequency instability was found in simulations at high Re and/or low AR. In the experiments, the two dimensional instability (F_T) was triggered by an external source which resulted in a constant value for the low frequency. However, in the simulations the low frequency was not constant and varied with Re and AR. This low frequency could be triggered by numerical error in the simulations. However, in the F2NI and F2 regimes where a secondary frequency was present in the far wake, no low frequencies were found in the frequency power spectrum analysis. It should be noted that for AR=1.00, no secondary frequencies were observed in the wake. This is likely due to the fact that, for circular cylinders, secondary structures develop at over 100 NDU downstream. At AR=1.00, the numerical diffusion in the simulation diffuses the wake structures so 2-dimensional instabilities are not amplified.

Using the frequency spectrum density to analyse the wake structures is a better method for developing the parameter space model since it allows clearer definition than flow visualisations. The tertiary frequency present in the wake is difficult to visualise and was only detected by analysing the frequency power spectrum. The inception point for the secondary frequency is also difficult to visualise because the Karman vortices have decayed before they interact with the 2-dimensional instability. However, visualisations are still very important and confirmed the presence of the low frequency in the wake.

Circular cylinders are used as the bench mark for simulations on bluff bodies. However, the associated flow structures do not encompass all the wake structures that are associated with bluff bodies. Other simple bluff bodies should also considered in order to fully understand the dynamics of bluff body wake structures.

Acknowledgements

The authors acknowledge the computing resources provided by VPAC and APAC for the numerical simulations.

References

[1] Cimbala, J.M., Nagib, H.M., Roshko, A., 1988, "Large structures in the far wake of two-dimensional bluff bodies." *Journal of Fluid Mechanics*, vol. 190, pp. 265.

[2] Johnson, S.A., Thompson, M.C. Hourigan, K., 2001, "Flow Past Elliptical Cylinders at Low Reynolds Numbers", *14th Australasian Fluid Mechanics Conference*, Adelaide

[3] Najjar F.M. & Balachandar, S., Low-frequency unsteadiness in the wake of a normal flat plate. *Journal of Fluid Mechanics,* 370, 1998, 101-147.

[4] Taneda, S., 1959, "Downstream development of wakes behind cylinder," *J. Phys, Soc, Jpn.*, Vol. 14, pp. 843.

[5] Thompson, M.C., Hourigan, K., Sheridan, J., Three-dimensional instabilities in the wake of a circular cylinder, *Experimental and Thermal Fluid Science,*12, 1996, 190-196.

[6] Williamson, C.H.K. and Prasad, A., 1993, "A new mechanism for oblique wave resonance in the 'natural' far wake," *Journal of Fluid Mechanics*, Vol. 256, pp 269-313.

[7] Williamson, C.H.K. and Prasad, A., 1993, "Oblique wave interactions in the far wake," *Physics of Fluids*, Vol. 5, pp. 1854-1857

[8] Williamson, C.H.K., 1992, "The natural and forced formation of spot-like 'vortex dislocations' in the transition of a wake" *Journal of Fluid Mechanics*, vol. 243 pp. 393.

[9] Williamson, C.H.K., Three-dimensional wake transition, 1996, *Journal of Fluid Mechanics*, 328, 1996, 345-407.